

Highly efficient adsorption of bulky dye molecules in waste water on
ordered mesoporous carbons

Xin Zhuang; **Ying Wan***; Cuimiao Feng; Ying Shen; Dongyuan Zhao

有序介孔碳作为高效吸附剂用于去除废水中大分子有机染料

中文摘要:

活性炭是最广泛使用的吸附剂之一。但其孔分布不均匀,难建立吸附剂结构、与吸附分子尺寸之间的关联模型。

本文通过溶剂挥发诱导自组装的方法合成了高比表面积有序介孔碳材料,并应用于吸附废水中的染料大分子。介孔碳材料对于大体积染料分子(亚甲基蓝,碱性品红,罗丹明 B, 灿烂黄, 维多利亚蓝 B, 甲基橙和苏丹红 G)的吸附量是商业活性炭(介孔率几乎为 100%, 比表面积 $1630 \text{ m}^2/\text{g}$)的两倍。介孔碳的优良吸附性能还表现在,对低浓度的染料有高达 99% 的吸附率,以及对碱性、酸性、偶氮染料均有优异的吸附性能。吸附剂经过洗脱后,仍然保持有序介观结构和高比表面积,可重复使用。为考察孔结构和吸附性能之间的关系,以酚醛树脂为碳源,三嵌段共聚物为结构导向剂,合成了具有不同孔尺寸、比表面积和孔体积的三种有序介孔碳材料。XRD、TEM 和 N_2 吸附脱附曲线等表征手段表明,三种介孔碳材料都具有高度有序的 2D 六方结构,高的比表面积($398\text{-}2580 \text{ m}^2/\text{g}$),大的孔体积($0.51\text{-}2.16 \text{ cm}^3/\text{g}$)和均一的孔径分布($4.5\text{-}6.4 \text{ nm}$)。通过比较其吸附量和估测孔隙占据率,发现染料分子的尺寸和介孔碳的孔径等因素,在有序介孔碳的吸附过程中起决定性作用,并据此初步提出了染料在介孔碳孔道内的吸附模式。三种介孔碳材料中,具有高比表面积($2580 \text{ m}^2/\text{g}$),大孔体积($2.16 \text{ cm}^3/\text{g}$)和双孔分布(6.4 nm 、 1.7 nm) 的有序介孔碳,对碱性大体积染料分子的吸附表现出最高吸附量。

Highly Efficient Adsorption of Bulky Dye Molecules in Wastewater on Ordered Mesoporous Carbons

Xin Zhuang,[†] Ying Wan,^{*,†} Cuimiao Feng,[†] Ying Shen,[†] and Dongyuan Zhao[‡]

Department of Chemistry, Shanghai Normal University, Shanghai 200234, P. R. China, and Department of Chemistry, Shanghai Key Laboratory of Molecular Catalysis and Innovative Materials, Fudan University, Shanghai 200433, P. R. China

Received October 9, 2008. Revised Manuscript Received December 15, 2008

We demonstrate, for the first time, the application of ordered mesoporous carbons with large pore sizes prepared from the surfactant-templating approach in efficient disposal of wastewater containing bulky dye molecules. The adsorption amount for the bulky dye (methylthionine chloride, fuchsin basic, rhodamine B, brilliant yellow, methyl orange, or Sudan G) is almost twice that of the activated carbon in which mesopores contribute almost 100% to the total surface area and volume. The ordered mesoporous carbon adsorbent has a high adsorption rate (>99.9%) for low-concentration dyes, good performance in decoloration regardless of the dye nature, including basic, acidic, or azo dyes, and high stability after dye elution. To establish the relationship between the pore texture and adsorption properties, three kinds of ordered mesoporous carbons with different pore sizes, surface areas, and pore volumes have been synthesized by using phenolic resins as carbon sources and triblock copolymer as a structure-directing agent. The XRD, TEM, and N₂ sorption measurements reveal that all mesoporous carbonaceous materials have the highly ordered 2D hexagonal mesostructure, high surface areas (398–2580 m²/g), large pore volumes (0.51–2.16 cm³/g), and uniform pore sizes ranging from 4.5 to 6.4 nm. The adsorption capacities are compared and the pore occupation is estimated to understand the adsorption behaviors in the ordered mesopores with different diameters and models. The spatial effect of dye molecules is the determinative factor for the adsorption in ordered mesoporous carbons with various pore textural properties. The mesoporous carbon with an extremely high surface area (2580 m²/g), a large pore volume (2.16 cm³/g), and bimodal pores (6.4 and 1.7 nm) prepared from the silica–carbon composite shows the highest adsorption capacities for bulky basic dyes among the three ordered mesoporous carbons.

1. Introduction

The effluents from textile plants contain portions of dyes, which are deeply colored, multicomponent, and low biodegradable, and have become one of the most serious pollutants in water. For example, most dyes have high tinctorial value, and less than 1 ppm of the dye produces an obvious coloration in water. Various treatments for the removal of dyes have been investigated, including adsorption,^{1–14} chemical coagulation,^{15–17} photodegradation,^{18–22} biodegradation,^{23,24}

active sludge,²⁵ etc. Among them, adsorption on porous carbons (mainly activated carbons, carbon blacks, and activated carbon fibers) is one of the most efficient processes for dye removal and decoloration,^{26–30} because of large specific surface areas, pore volumes, chemical inertness, and

* To whom correspondence should be addressed. Tel: 86-21-6432-2516. Fax: 86-21-6432-2511. E-mail: ywan@shnu.edu.cn.

[†] Shanghai Normal University.

[‡] Fudan University.

- (1) Robinson, T.; Chandran, B.; Nigam, P. *Water Res.* **2002**, *36*, 2824.
- (2) Namasivayam, C.; Kavitha, D. *Dyes Pigment.* **2002**, *54*, 47.
- (3) Wong, Y. C.; Szeto, Y. S.; Cheung, W. H.; McKay, G. *Langmuir* **2003**, *19*, 7888.
- (4) Orthman, J.; Zhu, H. Y.; Lu, G. Q. *Sep. Purif. Technol.* **2003**, *31*, 53.
- (5) Chiou, M. S.; Li, H. Y. *Chemosphere* **2003**, *50*, 1095.
- (6) Ho, K. Y.; McKay, G.; Yeung, K. L. *Langmuir* **2003**, *19*, 3019.
- (7) Dogan, M.; Alkan, M. *Chemosphere* **2003**, *50*, 517.
- (8) Blackburn, R. S. *Environ. Sci. Technol.* **2004**, *38*, 4905.
- (9) Allen, S. J.; McKay, G.; Porter, J. F. *J. Colloid Interface Sci.* **2004**, *280*, 322.
- (10) Campbell, V. E.; Chiarelli, P. A.; Kaur, S.; Johal, M. S. *Chem. Mater.* **2005**, *17*, 186.
- (11) Aksu, Z.; Tezer, S. *Process Biochem.* **2005**, *40*, 1347.
- (12) Yan, Y. M.; Zhang, M. N.; Gong, K. P.; Su, L.; Guo, Z. X.; Mao, L. Q. *Chem. Mater.* **2005**, *17*, 3457.
- (13) Hu, Q. H.; Qiao, S. Z.; Haghsresht, F.; Wilson, M. A.; Lu, G. Q. *Ind. Eng. Chem. Res.* **2006**, *45*, 733.

- (14) Crini, G.; Peindy, H. N.; Gimbert, F.; Robert, C. *Sep. Purif. Technol.* **2007**, *53*, 97.
- (15) Lin, S. H.; Lin, C. M. *Water Res.* **1993**, *27*, 1743.
- (16) Kim, T. H.; Park, C.; Yang, J. M.; Kim, S. J. *Hazard. Mater.* **2004**, *112*, 95.
- (17) Canizares, P.; Martinez, F.; Jimenez, C.; Lobato, J.; Rodrigo, M. A. *Environ. Sci. Technol.* **2006**, *40*, 6418.
- (18) Vinodgopal, K.; Bedja, I.; Kamat, P. V. *Chem. Mater.* **1996**, *8*, 2180.
- (19) Tang, W. Z.; Zhang, Z.; An, H.; Quintana, M. O.; Torres, D. F. *Environ. Technol.* **1997**, *18*, 1.
- (20) Lachheb, H.; Puzenat, E.; Houas, A.; Ksibi, M.; Elaloui, E.; Guillard, C.; Herrmann, J. M. *Appl. Catal., B* **2002**, *39*, 75.
- (21) Zhao, J. C.; Chen, C. C.; Ma, W. H. *Top. Catal.* **2005**, *35*, 269.
- (22) Chen, C. C.; Wang, Q.; Lei, P. X.; Song, W. J.; Ma, W. H.; Zhao, J. C. *Environ. Sci. Technol.* **2006**, *40*, 3965.
- (23) RazoFlores, E.; Luijten, M.; Donlon, B. A.; Lettinga, G.; Field, J. A. *Environ. Sci. Technol.* **1997**, *31*, 2098.
- (24) Kornaros, M.; Lyberatos, G. J. *Hazard. Mater.* **2006**, *136*, 95.
- (25) Lindberg, R. H.; Olofsson, U.; Rendahl, P.; Johansson, M. I.; Tysklind, M.; Andersson, B. A. V. *Environ. Sci. Technol.* **2006**, *40*, 1042.
- (26) Meshko, V.; Markovska, L.; Mincheva, M.; Rodrigues, A. E. *Water Res.* **2001**, *35*, 3357.
- (27) Tanthapanichakoon, W.; Ariyadejwanich, P.; Japthong, P.; Nakagawa, K.; Mukai, S. R.; Tamon, H. *Water Res.* **2005**, *39*, 1347.
- (28) Walker, G. M.; Weatherley, L. R. *Water Res.* **1997**, *31*, 2093.
- (29) Walker, G. M.; Weatherley, L. R. *Environ. Pollut.* **1998**, *99*, 133.
- (30) Tamai, H.; Yoshida, T.; Sasaki, M.; Yasuda, H. *Carbon* **1999**, *37*, 983.

good mechanical stability of carbon. In particular, activated carbon can efficiently treat dyes in wastewater that show difficulty in biodegradation, e.g., azo dyes. However, the practical applications of these porous carbons are restricted because of micropore sizes. For example, Walker et al.³¹ studied the adsorption behavior of three kinds of acidic dyes on activated carbon. Only 14% of pores can be occupied by the dyes. The low utility of pores is more distinct in the adsorption of molecules with larger diameters. In addition, the adsorption amount of phenol, iodine, or tannic acid on activated carbon increases with the increase of mesopore volumes.³² Most micropores in activated carbon are inaccessible. Therefore, lots of methods have been applied to increase mesopore volumes, including adding metal salt,³³ erosion by acid or base,³⁴ ammonia sweeping,^{35,36} low-pressure plasma,³⁷ oxygen plasma,³⁸ and high-temperature treatment;³⁹ but carbons with wide pore-size distributions are always produced. This feature restricts the establishment of the relationship between the pore texture and adsorption properties. The surface chemistry of activated carbon, in particular from different sources and from different treatments, is uncertain.⁴⁰ Because the adsorption capacity of a given carbon strongly depends on the chemical nature of the surface,⁴¹ the adsorption performance for the same dye differ from each other. The sorption behavior cannot be identically compared. Although much has been accomplished in terms of sorption properties, much work is still necessary to identify the sorption clearly,⁴¹ especially on the basis of the same carbon source. Activated carbon also has a problem in the adsorption of low-concentration dyes.^{42,43} Therefore, mesoporous carbons with uniform pores that are derived from a certain carbon sources, and can be directly used without any treatment, are desirable for the adsorption of bulky organic dyes.

Ordered mesoporous carbons possess unique structures, high surface areas, and large and tunable pore channels, showing advantages in adsorption, separation, catalysis, and electrodes and in particular for the large-molecule-involved processes. These carbons are normally fabricated by the nanocasting process.^{44–59} Mesoporous silica is chosen as a hard template. The carbon source is then filled inside the mesopores. Upon carbonization and subsequent removal of the silica scaffold by HF or NaOH solution, ordered

mesoporous carbon is produced. For example, Hartmann et al.⁴⁸ found that the mesoporous carbon replica showed a larger adsorption amount of vitamin E than activated carbon. Vinu et al.^{57,58} investigated the adsorption of L-histidine and lysozyme on different adsorbents and found a much higher ability for amino acid on the mesoporous carbon replica than mesoporous silica because of the hydrophobic interaction between the carbon adsorbent and the adsorbate. In addition, the mesoporous carbon adsorbent with a large pore size and pore volume results in a high adsorption quality for protein.⁵⁸ Hyeon and co-workers⁶⁰ synthesized nanoporous carbons with extremely high mesopore volumes and surface areas using silica nanoparticles as templates. These nanoporous carbons exhibit excellent adsorption capacities for bulky dyes. More recently, several groups developed the direct synthesis method for ordered mesoporous carbons from the self-assembly of amphiphilic block copolymers and phenolic resins.^{61–69} A thin film containing hydrophilic poly(4-vinylpyridine) and resorcinol domains and hydrophobic polystyrene domains can self-assemble an ordered hexagonal mesostructure. After polymerization with the formaldehyde vapor and carbonization, mesoporous carbon thin films were produced by Dai and co-workers.⁶¹ Meng et al.^{63,65} used all commercially available, low-cost raw materials, namely, phenol, formaldehyde, and triblock copolymer F127, to prepare highly ordered mesoporous carbon powders with uniform pore sizes ranging from 3 to 8 nm. This simple operation facilitates the large-scale production of ordered

(31) Walker, G. M.; Weatherley, L. R. *Chem. Eng. J.* **2001**, *83*, 201.

(32) Hsieh, C. T.; Teng, H. S. *Carbon* **2000**, *38*, 863.

(33) Takeuchi, Y.; Itoh, T. *Sep. Technol.* **1993**, *3*, 168.

(34) Vinke, P.; Vandereijk, M.; Verbree, M.; Voskamp, A. F.; Vanbekkum, H. *Carbon* **1994**, *32*, 675.

(35) Boudou, J. P.; Chehimi, M.; Broniek, E.; Siemieniowska, T.; Bimer, J. *Carbon* **2003**, *41*, 1999.

(36) Mangun, C. L.; Benak, K. R.; Economy, J.; Foster, K. L. *Carbon* **2001**, *39*, 1809.

(37) Tang, S.; Lu, N.; Wang, J. K.; Ryu, S. K.; Choi, H. S. *J. Phys. Chem. C* **2007**, *111*, 1820.

(38) Garcia, A. B.; Martinez-Alonso, A.; Leon, C.; Tascon, J. M. D. *Fuel* **1998**, *77*, 613.

(39) Qiao, Z. J.; Li, J. J.; Zhao, N. Q.; Wei, N. *New Carbon Mater.* **2004**, *19*, 53.

(40) Wibowo, N.; Setyadhi, L.; Wibowo, D.; Setiawan, J.; Ismadji, S. J. *Hazard. Mater.* **2007**, *146*, 237.

(41) Crini, G. *Bioresour. Technol.* **2006**, *97*, 1061.

(42) Mohamed, M. M. *J. Colloid Interface Sci.* **2004**, *272*, 28.

(43) Singh, K. P.; Mohan, D.; Sinha, S.; Tondon, G. S.; Gosh, D. *Ind. Eng. Chem. Res.* **2003**, *42*, 1965.

(44) Ryoo, R.; Joo, S. H.; Jun, S. *J. Phys. Chem. B* **1999**, *103*, 7743.

(45) Ryoo, R.; Joo, S. H.; Kruk, M.; Jaroniec, M. *Adv. Mater.* **2001**, *13*, 677.

(46) Lee, J.; Yoon, S.; Hyeon, T.; Oh, S. M.; Kim, K. B. *Chem. Commun.* **1999**, 2177.

(47) Lee, J.; Yoon, S.; Oh, S. M.; Shin, C. H.; Hyeon, T. *Adv. Mater.* **2000**, *12*, 359.

(48) Hartmann, M.; Vinu, A.; Chandrasekar, G. *Chem. Mater.* **2005**, *17*, 829.

(49) Kruk, M.; Jaroniec, M.; Ryoo, R.; Joo, S. H. *J. Phys. Chem. B* **2000**, *104*, 7960.

(50) Darmstadt, H.; Roy, C.; Kaliaguine, S.; Choi, S. J.; Ryoo, R. *Carbon* **2002**, *40*, 2673.

(51) Vinu, A.; Streb, C.; Murugesan, V.; Hartmann, M. *J. Phys. Chem. B* **2003**, *107*, 8297.

(52) Lu, A. H.; Li, W. C.; Schmidt, W.; Schuth, F. *Microporous Mesoporous Mater.* **2005**, *80*, 117.

(53) Yang, H. F.; Zhao, D. Y. *J. Mater. Chem.* **2005**, *15*, 1217.

(54) Han, S. J.; Kim, M.; Hyeon, T. *Carbon* **2003**, *41*, 1525.

(55) Lee, J.; Han, S.; Hyeon, T. *J. Mater. Chem.* **2004**, *14*, 478.

(56) Kim, T. W.; Ryoo, R.; Gierszal, K. P.; Jaroniec, M.; Solovyov, L. A.; Sakamoto, Y.; Terasaki, O. *J. Mater. Chem.* **2005**, *15*, 1560.

(57) Vinu, A.; Hossain, K. Z.; Kumar, G. S.; Ariga, K. *Carbon* **2006**, *44*, 530.

(58) Vinu, A.; Miyahara, M.; Ariga, K. *J. Phys. Chem. B* **2005**, *109*, 6436.

(59) Wan, Y.; Yang, H. F.; Zhao, D. Y. *Acc. Chem. Res.* **2006**, *39*, 423.

(60) Han, S. J.; Sohn, K.; Hyeon, T. *Chem. Mater.* **2000**, *12*, 3337.

(61) Liang, C. D.; Hong, K. L.; Guiochon, G. A.; Mays, J. W.; Dai, S. *Angew. Chem., Int. Ed.* **2004**, *43*, 5785.

(62) Tanaka, S.; Nishiyama, N.; Egashira, Y.; Ueyama, K. *Chem. Commun.* **2005**, 2125.

(63) Meng, Y.; Gu, D.; Zhang, F. Q.; Shi, Y. F.; Yang, H. F.; Li, Z.; Yu, C. Z.; Tu, B.; Zhao, D. Y. *Angew. Chem., Int. Ed.* **2005**, *44*, 7053.

(64) Liang, C. D.; Dai, S. *J. Am. Chem. Soc.* **2006**, *128*, 5316.

(65) Meng, Y.; Gu, D.; Zhang, F. Q.; Shi, Y. F.; Cheng, L.; Feng, D.; Wu, Z. X.; Chen, Z. X.; Wan, Y.; Stein, A.; Zhao, D. Y. *Chem. Mater.* **2006**, *18*, 4447.

(66) Liu, R. L.; Shi, Y. F.; Wan, Y.; Meng, Y.; Zhang, F. Q.; Gu, D.; Chen, Z. X.; Tu, B.; Zhao, D. Y. *J. Am. Chem. Soc.* **2006**, *128*, 11652.

(67) Wan, Y.; Shi, Y. F.; Zhao, D. Y. *Chem. Commun.* **2007**, 897.

(68) Wan, Y.; Shi, Y. F.; Zhao, D. Y. *Chem. Mater.* **2008**, *20*, 932.

(69) Wan, Y.; Qian, X.; Jia, N. Q.; Wang, Z. Y.; Li, H. X.; Zhao, D. Y. *Chem. Mater.* **2008**, *20*, 1012.

mesoporous carbons and their practical application in the adsorption of bulky dyes in polluted water.

Here, we demonstrate for the first time that ordered mesoporous carbons derived from phenolic resins can be utilized in efficient removal of bulky dyes from water. The mesoporous carbon with an extremely high surface area (2580 m²/g), large pore volume (2.16 cm³/g), and large bimodal pores (6.4 and 1.7 nm) shows about twice adsorption capacities for bulky dyes (methylthionine chloride, fuchsin basic, rhodamine B, brilliant yellow, methyl orange, and Sudan G) on comparison with commercial activated carbon. The mesoporous carbon adsorbent has a high adsorption rate (>99.9%) for low-concentration dyes, good performance in decoloration, and high stability after dye elution. To clarify the effects of pore texture and dye molecular size on adsorption, the adsorption capacities on bulky basic dyes are compared on the basis of three kinds of mesoporous carbons, which are derived from the same phenolic resins precursors, and have the same 2D hexagonal structure but different pore sizes, surface areas, and pore volumes. The spatial effect of dye molecules is found to be the determinative factor for the adsorption in carbons with different pore sizes, surface areas, and pore volumes. These behaviors offer good opportunities for mesoporous carbons in adsorption of organic pollutants in wastewater.

2. Experimental Section

2.1. Chemicals. Poly(propylene oxide)-*b*-poly(ethylene oxide)-*b*-poly(propylene oxide) triblock copolymer Pluronic F127 (EO₁₀₆PO₇₀EO₁₀₆, $M_w = 12\,600$) was purchased from Acros Chemical Inc. Other chemicals were purchased from Shanghai Chemical Corp. All chemicals were used as received without any further purification. Water used in all syntheses was distilled and deionized. Activated carbon was supplied by Xinzhuang Activated Carbon Company of Shanghai. Before use, it was boiled in hot KOH solution (10 wt %) at 100 °C for about 4 h and the treatment was repeated five times. Finally, the carbon powders were calcined at 900 °C for 4 h under nitrogen.

2.2. Preparation of Mesoporous Carbons. The mesoporous carbons were prepared by using the surfactant-templating method with phenol and formaldehyde as carbon sources and triblock copolymer F127 as a structure-directing agent according to the references.^{65,66} Phenol and formaldehyde were first prepolymerized under basic conditions to form water- and ethanol-soluble phenolic resins (see details in the Supporting Information). The synthesis procedure for the ordered mesoporous carbon (MPC) was as following. First, 2.54 g of triblock copolymer F127 was dissolved in 30.0 g of ethanol to obtain a clear solution. To it was added 15.0 g of 20 wt% phenolic resins ethanolic solution (containing 1.83 g of phenol and 1.17 g of formaldehyde). After being stirred for 10 min, the mixture was poured into dishes. The dishes were then placed in a hood to evaporate ethanol at ambient temperature for 8 h, and in an oven to thermopolymerize at 100 °C for 24 h in sequence. The template-Bakelite composites were taken from the dishes, loaded in several quartz boats, and put in a tubular furnace that was protected by nitrogen. Heating programs were from ambient temperature to 350 °C with a rate of 1 °C/min, keeping this temperature for 5 h to remove the triblock copolymer template, from 350 to 900 °C with a rate of 1 °C/min, and keeping this temperature for 4 h to carbonize. The black powders were collected. The synthesis for the mesoporous silica-carbon composite (MPSC) was similar to the

above procedure, except the addition of prehydrolyzed TEOS in the mixture containing preformed phenolic resins, triblock copolymer F127, and ethanol. TEOS (2.08 g) was prehydrolyzed in the presence of 1.0 g of HCl (0.2 M) and 4.0 g of ethanol. This mixture was then added to the solution containing 5.0 g of 20 wt% preformed phenolic resin, 1.6 g of F127, and 8.0 g of ethanol. The subsequent treatment was exactly the same as the above program. The mesoporous carbon MPSC/C was recovered after dissolution of the silica component in MPSC by 10 wt % HF solution at room temperature, filtration, washing with water and drying at 100 °C. The complete removal of silica component can be confirmed by the thermogravimetry analysis (TG, see Figure S1 in the Supporting Information). The ash contents of the mesoporous carbon MPC and MPSC/C (after the silica dissolution from MPSC) are undetectable, indicating pure carbon frameworks and the complete elimination of the silica component in MPSC/C. The curve of the MPSC adsorbent features a middle weight loss of about 42%, in the range between 450 and 700 °C, indicating that the weight ratio for carbon and silica in the nanocomposite is about 1:1.2.

2.3. Characterization. The small-angle X-ray diffraction (XRD) measurements were taken on a Rigaku D/max B diffractometer using Cu K α radiation (40 kV, 20 mA). The *d*-spacing values were calculated by the formula of $d = 0.15408/2\sin\theta$, and the unit-cell parameters were calculated from the formula of $a_0 = 2d_{100}/\sqrt{3}$. N₂ adsorption-desorption isotherms were measured at 77 K with a Quantachrome NOVA 4000 e analyzer. The Brunauer-Emmett-Teller (BET) method was utilized to calculate the specific surface areas (S_{BET}). By using the Barrett-Joyner-Halenda (BJH) model, the pore volumes and pore size distributions were derived from the adsorption branches of isotherms. The micropore volumes (V_m) and micropore surface areas were calculated from the *V*-*t* plot method. The *t* values were calculated as a function of the relative pressure using the de Boer equation, $t \text{ (nm)} = [0.1399/(\log(p_0/p) + 0.0340)]^{1/2}$. V_m was obtained using the equation of $V_m \text{ (cm}^3\text{/g)} = 0.001547I$, where *I* represents the *Y* intercept in the *V*-*t* plot. Transmission electron microscopy (TEM) experiments were conducted on a JEOL 2011 microscope operated at 200 kV. The samples for TEM measurements were suspended in ethanol and supported onto a holey carbon film on a Cu grid. Weight losses and the associated temperatures were determined by thermogravimetry analysis with a Mettler Toledo TG/SDTA 851e apparatus. Samples were heated from room temperature to 1000 °C at a rate of 10 °C/min in air flow.

2.4. Batch Mode Adsorption. The batch mode adsorption studies for various dyes, including methylthionine chloride (MC), fuchsin basic (FB), rhodamine B (RB), brilliant yellow (BY), victoria blue B (VB), methyl orange (MO), and Sudan G (SG), were carried out by agitating 0.02 g of ordered mesoporous carbons in 50 mL of dye solution. For comparison, activated carbon was also tested as an adsorbent. Table 1 gives the concentration of each dye solution. All dyes were dissolved in deionized water except for Sudan G in ethanol. The mixture was continuously shaken in a shaking bath with a speed of 120 rpm at 30 °C until the equilibrium was reached (typically 24 h). After adsorption, an aliquot was centrifuged at 3000 rpm for 3 min and the dye concentration in the clear supernatant was determined using a XinMao Ultraviolet-visible (UV-vis) spectrophotometer (UV-7504 PC). The wavenumber for the detection is listed in Table 1. The equilibrium adsorption capacities (Q_e) and the molar adsorption capacities (Q_m) were determined according to the following formula

$$Q_e = (C_i - C_e)V/m$$

$$Q_m = Q_e/M$$

wherein C_i is the initial concentration, C_e is the residual or equilibrium concentration, V is the volume of the liquid phase, m is the mass of the adsorbent, and M is the molecular weight of the dyes. The estimated adsorbed volume V_{ads}' of dyes in mesoporous carbons was calculated on the basis of the following formula

$$V_{ads}' = Q_m N_A V_{dye}$$

wherein N_A is the Avogadro's number, and V_{dye} is the volume for each dye estimated from the Newtonian ball and spring model (Table 1). The sample after dye adsorption was named as CARBON-DYE. For example, MPC-MC means the MPC sample after adsorption of methylthionine chloride (MC).

To study the effect of contacting time on adsorption, we continuously shook the mixture containing ordered mesoporous carbon and dye for different times, centrifuged it for 3 min, and analyzed it. The contacting time was counted from the mixing of carbon with dye to the suction of the clear supernatant.

2.5. Desorption. Desorption of methylthionine chloride was carried out by using 0.02 g of used MPSC/C loaded with about 15 mg of dye in 50 mL of distilled water, 1.0 M H_2SO_4 , and 50% (V/V) acetic acid, respectively.

2.6. Decoloration. 0.02 g of mesoporous carbon MPSC/C was added into a 50 mL of solution containing 0.25 mg of dye (methylthionine chloride, fuchsin basic, and methyl orange). After 1 min, the mixture was centrifuged at 3000 rpm for 3 min.

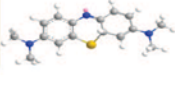
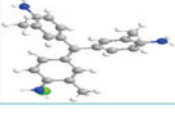
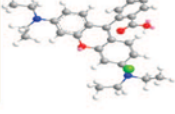
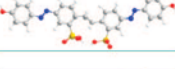
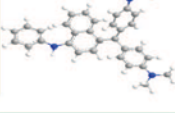
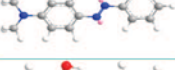
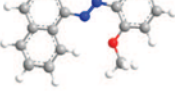
2.7. Low-Concentration Adsorption. Low-concentration adsorption studies for methylthionine chloride, fuchsin basic, and methyl orange were carried out by agitating 0.02 g of mesoporous carbon MPSC/C adsorbent in 50 mL of the dye solution. The concentration of each dye solution was 5 and 10 ppm, respectively. The adsorption test was the same as the batch mode except that the adsorption time was shortened to 3 h.

3. Results

3.1. Physical and Chemical Properties of the Adsorbents. The ordered mesoporous carbons with different pore sizes, surface areas, and pore volumes were synthesized via the surfactant self-assembling approach by using preformed phenolic resins as carbon sources and triblock copolymer F127 as a structure-directing agent. Among the products, MPC is the pure carbon; MPSC is the silica-carbon nanocomposite in which the silica precursor is added in the initial solution; and MPSC/C is the descendant of MPSC by etching the silica component, and hence is made of pure carbon.

The small-angle XRD pattern (Figure 1) for the MPC adsorbent reflects the 2D hexagonal mesostructure with a cell parameter of 9.7 nm. MPSC possesses the similar diffraction pattern with MPC, indicating that MPSC also has a highly ordered hexagonal mesostructure and the cell parameter increases to 12.1 nm. The XRD pattern of the

Table 1. Newtonian Ball and Spring Model, Molecular Size, Concentration of Solution, and Wavenumber for the UV Absorption for Each Dye

Dye	Newtonian ball and spring model	Molecular size (nm)	Molecular weight (g/mol)	Nature	Concentration (g/L)	UV Absorption (nm)
Methylthionine chloride		1.26×0.77×0.65	320	basic	0.005 - 0.9	665
Fuchsin basic		1.06×1.05×0.48	338	basic	0.4	543
Rhodamine B		1.59×1.18×0.56	478	basic	0.4	554
Brilliant yellow		2.45×1.09×0.36	625	basic azo	0.4	400
Victoria blue B		1.47×1.41×0.44	506	basic	0.4	603
Methyl orange		1.31×0.55×0.18	327	acidic azo	0.4	465
Sudan G		1.31×0.84×0.24	278	acidic azo	0.4	502

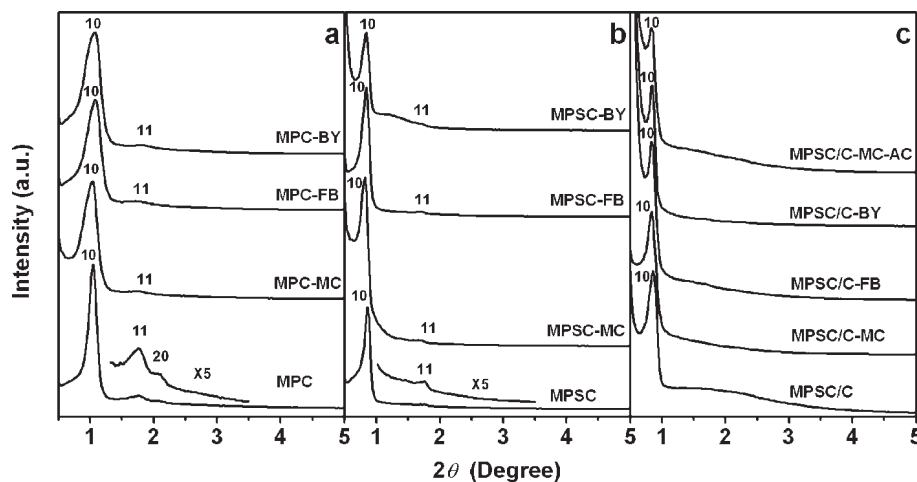


Figure 1. XRD patterns for fresh mesoporous carbons prepared from the surfactant-templating method and these carbons after adsorption of methylthionine chloride (MC), fuchsin basic (FB), and brilliant yellow (BY): (a) mesoporous carbon (MPC), (b) mesoporous silica-carbon composite (MPSC), (c) mesoporous silica-carbon composite derived carbon (MPSC/C). The suffix in the name represents the adsorbing dye. For example, MPC-MC represents the mesoporous carbon MPC adsorbent after adsorption of MC. The curve in (c) labeled as MPSC/C-MC-AC represents the MPSC sample after adsorption with MC and subsequent elution with acetic acid.

mesoporous carbon MPSC/C from the silica-carbon composite exhibits a sharp diffraction peak corresponding to a repeat distance of 12.1 nm, the same as that of its mother MPSC. TEM images (Figure 2) of all mesoporous carbons show stripelike and hexagonally arranged pores, further confirming the ordered 2D hexagonal mesostructure. Although the XRD diffraction peaks in the range of $1.5\text{--}3^\circ$ for MPSC/C are not as resolved as the other two mesoporous carbons, TEM images exhibit ordered mesostructure in large domains. No distinct defect is observed.

Ordered mesoporous carbonaceous materials MPC, MPSC and MPSC/C show the type IV shape of nitrogen adsorption isotherms (Figure 3), characteristic of nanostructured materials with uniform mesopores. Remarkably, a distinctly increased adsorption at the relative pressure of p/p_0 of 0.1–0.3 is observed for MPSC/C (Figure 3c), suggesting small pores below 3.5 nm. The textual properties of the different carbon adsorbents are compiled in Table 2. MPC has a pore volume of $0.55\text{ cm}^3/\text{g}$ and a BET surface area of $757\text{ m}^2/\text{g}$. The BJH pore-size distribution curve shows a uniform distribution, centered at 4.5 nm (Figure 4a). The t -plot analysis (see Figure S2a in the Supporting Information) reveals that the high BET surface area and pore volume for the MPC adsorbent mainly result from microporosity, caused by the oxidation of polymer or carbon species. The BET surface area and pore volume of MPSC are as low as $398\text{ m}^2/\text{g}$ and $0.51\text{ cm}^3/\text{g}$, respectively, but the pore size increases to 6.4 nm. This sample has a micropore surface area of $71\text{ m}^2/\text{g}$. Almost total surface area and pore volume are contributed by mesopores that are generated by removal of triblock copolymer. It should be noted that the primary mesopore diameter in MPSC is larger than that in MPC, although the same triblock-copolymer F127 is used in the syntheses. This phenomenon can be explained by the addition of inorganic rigid silica component in MPSC, which can efficiently resist the framework shrinkage during the high-temperature carbonization,⁷⁰ in good agreement with the increased domain size. Interestingly, the MPSC/C adsorbent possesses an extremely high BET surface area of $2580\text{ m}^2/\text{g}$

g, a large pore volume of $2.16\text{ cm}^3/\text{g}$, and a bimodal-like pore-size distribution with the most probable pore sizes of 6.4 and 1.7 nm. The primary mesopore size is the same as its mother MPSC, whereas the secondary one is much smaller. On the basis of the t -plot analysis (see Figure S2c in the Supporting Information), and the mesopore surface area of MPSC with the same primary mesopore size as MPSC/C, the contribution of micropores and primary mesopores to the total BET surface area is about 0 and 13%, respectively. Therefore, the majority of the surface area (87%) is arisen from the secondary mesopores, which is reflected by the bimodal pore-size distribution centered at 1.7 nm. Recalling that the mesoporous carbon MPSC/C is a product by etching silica from the MPSC nanocomposite, the primary mesopores are inherited from the mother by eliminating the triblock copolymer template, and the secondary small mesopores are more likely generated by the removal of silica component in the carbonaceous framework. The mild treatment by 10% HF solution shows a minor effect on the primary mesopores and the mesostructure, only leaving plenty of voids inside the framework. These secondary mesopores are interpenetrated and accessible because of the fact that the silica and carbon components are well-dispersed inside the whole framework.⁶⁶ A scheme for the generation of the secondary mesopores are shown in Figure S3 in the Supporting Information. Therefore, the weak diffractions at higher angles in the small-angle XRD patterns are possibly due to the voids inside the carbon pore walls, which are generated by etching silica in the silica-carbon pore wall. The N_2 sorption isotherms for activated carbon are shown in Figure S4 in the Supporting Information. The BET surface area and pore volume are $1663\text{ m}^2/\text{g}$ and $1.45\text{ cm}^3/\text{g}$, respectively, to which mesopore (size ranging from 1.5 to 30 nm) surface area and volume contribute almost 100% (micropore surface area and volume are negligible on the basis of the t -plot analysis).

(70) Wei, Y.; Jin, D. L.; Yang, C. C.; Wei, G. J. *Sol-Gel Sci. Technol.* **1996**, 7, 191.

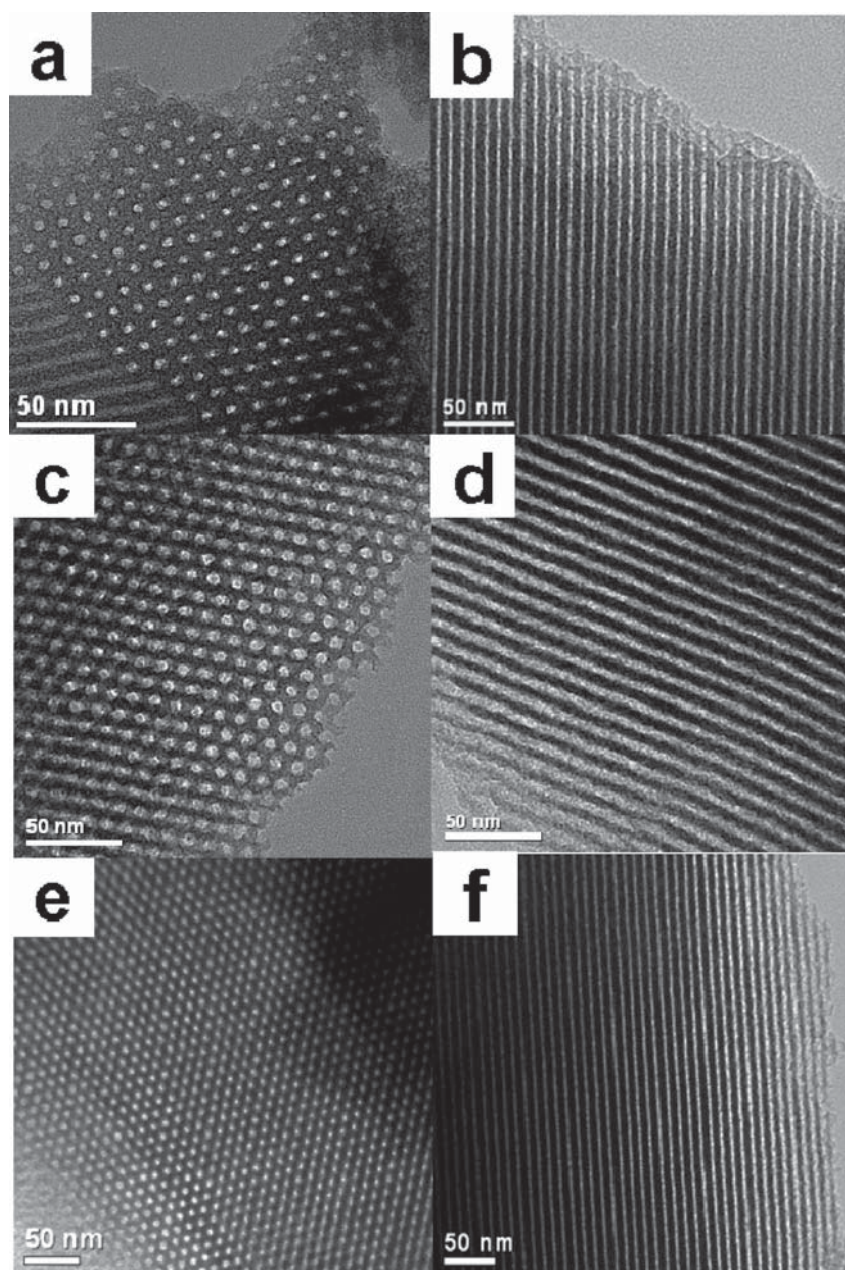


Figure 2. TEM images for mesoporous carbons viewed from the directions parallel (a, c, e) and perpendicular (b, d, f) to the pore channels: (a, b) MPC, (c, d) MPSC, and (e, f) MPSC/C.

3.2. Adsorption Properties for Dyes. The adsorption of methylthionine chloride (MC), fuchsin basic (FB), rhodamine B (RB), brilliant yellow (BY), victoria blue B (VB), methyl orange (MO), and Sudan G (SG) were studied on the ordered mesoporous carbon MPSC/C (Table 3). For comparison, mesoporous activated carbon after treatment with KOH was also used as an adsorbent. The mesoporous carbon MPSC/C with bimodal pores exhibits high capacities in adsorbing multiple bulky dyes up to 785 mg/g (Table 3), including acidic dyes such as MO and SG, basic dyes such as MC, FB, RB, BY, and VB, and azo dyes such as MO, SG, and BY. These values are almost one time higher than those on the mesoporous activated carbon, except for large VB molecules the adsorption capacity of which is similar on these two carbons. The adsorption capacities over other activated carbons in literatures are listed in Table S1 in the Supporting Information and are lower than those on the MPSC/C

adsorbent, although particular treatments for activated carbons and the adjustment for the pH value are adopted.^{71–73} In the present adsorption, the mesoporous carbon is directly added into wastewater without any treatment and the adjustment for the pH value. These results reflect that MPSC/C is a highly efficient adsorbent for bulky dyes.

The efficient adsorption for dyes was also studied for the adsorption of low-concentration dye and decoloration of water. The adsorption of dyes with a low concentration is extremely important, because this value is a decisive factor for the residue concentration of dyes in water. The adsorption of MC, FB, and MO with the concentrations of 5 and 10

(71) Hameed, B. H.; Din, A. T. M.; Ahmad, A. L. *J. Hazard. Mater.* **2007**, *141*, 819.

(72) Attia, A. A.; Girgis, B. S.; Khedr, S. A. *J. Chem. Technol. Biotechnol.* **2003**, *78*, 611.

(73) Kumar, K. V.; Sivanesan, S. *J. Hazard. Mater.* **2006**, *129*, 147.

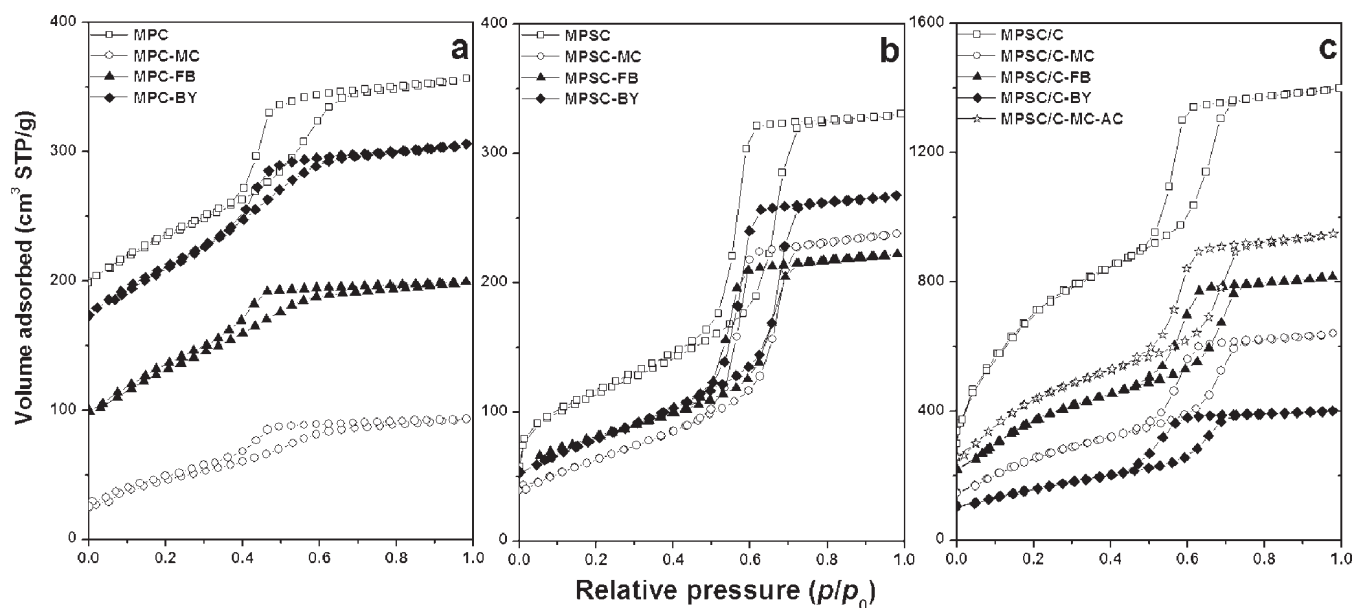


Figure 3. (a) Nitrogen sorption isotherms for the ordered mesoporous carbon MPC adsorbent before and after adsorption of MC, FB, and BY dyes; (b) the MPSC adsorbent before and after adsorption of dyes; (c) and the MPSC/C adsorbent before and after adsorption of dyes, and after subsequent dilution by acetic acid.

Table 2. Structural and Textual Properties of Ordered Mesoporous Carbons before and after Dye Adsorption

adsorbent ^a	a_0 (nm)	S_{BET} (m ² /g)	$S_{\text{BET}}^{\text{micro}}$ (m ² /g)	V_t (cm ³ /g)	V_m^{micro} (cm ³ /g)	D_p (nm)
MPC	9.7	757	396	0.55	0.21	4.5
MPC-MC	9.7	168	0	0.15	0	4.2
MPC-FB	9.6	450	81	0.31	0.05	3.1
MPC-BY	9.6	687	293	0.47	0.16	3.1
MPSC	12.1	398	71	0.51	0.04	6.4
MPSC-MC	12.3	233	0	0.37	0	6.4
MPSC-FB	12.1	239	0	0.37	0	6.4
MPSC-BY	12.1	284	8	0.41	0.01	6.3
MPSC/C	12.1	2580	0	2.16	0	6.4
MPSC/C-MC	12.3	937	0	0.99	0	6.4
MPSC/C-FB	12.2	594	0	0.71	0	6.4
MPSC/C-BY	12.2	573	0	0.62	0	5.9

^a The suffix in the sample name represents the adsorbed dye.

ppm was tested on the mesoporous carbon MPSC/C. The adsorption rates for all cases are higher than 99.9%, suggesting a complete removal. It may pave a way for the practical use. Optical photographs were taken before and after dye adsorption (Figure 5). For example, after the adsorption of various dyes (MC, FB and MO) with an initial concentration of 5 ppm on MPSC/C, the polluted water become clear and colorless, regardless of the initial color, ranging from blue (MC), pink (FB) to orange (MO), and the nature, including acidic (MO), basic (MC and FB), and azo (MO) dyes. This phenomenon further reveals the efficient adsorption and distinct decoloration for tinctorial wastewater by the ordered mesoporous carbon adsorbent.

To understand the adsorption on the carbon adsorbent and establish the relationship between the pore textual properties and the adsorption ability, the adsorption of basic bulky dyes on ordered mesoporous carbons that are derived from the same phenolic resins precursors and have different pore sizes, surface areas, and pore volumes was also investigated. The adsorbents were used without any further treatment. Figure 6 shows the equilibrium adsorption isotherms of MC on various mesoporous carbonaceous adsorbents (MPC, MPSC,

and MPSC/C). The isotherms belong to type I curve, characteristic of Langmuir isotherms. The amount of adsorbed MC dramatically increase at a lower final solution concentration, suggesting a high affinity between the dye molecule and the carbonaceous adsorbent surface;⁵⁷ the adsorbed amount reaches a plateau at a higher equilibrium solution concentration, reflecting the saturated adsorption. An order for the adsorption capacity of MC with a small molecular size on different adsorbents in the range of the equilibrium concentration is as follows: MPSC/C > MPC > MPSC. Figure 7 plots the adsorption capacities for MC (concentration: 0.4 g/L) over various materials as a function of the contacting time. A predominant increase in the initial period is found, indicating a fast adsorption. For example, the adsorption of MC inside mesochannels of MPSC/C in the first 10 min can reach 85% of the total amount. This phenomenon gives further evidence on the high affinity between the adsorbate and the adsorbent. The adsorption amount with a long contact time (24 h) is on the same order as above for the three ordered mesoporous carbonaceous materials.

Table 3 compiles the adsorption capacities for different dyes (concentration, 0.4 g/L; contacting time, 24 h) over various carbonaceous materials. The mesoporous silica-carbon composite MPSC exhibits lower adsorption capacities than MPSC/C, such as 371, 281, 139, and 106 mg/g for FB, RB, BY, and VB, respectively. In the adsorption of FB and RB with relatively large sizes, MPC shows the lowest capacities (207 and 215 mg/g) among the three ordered mesoporous carbons, although it shows a higher adsorption amount (540 mg/g) for the small-molecule-size MC than MPSC (384 mg/g). The adsorption quantities for large-molecular-size dyes such as BY and VB on MPC are close to those on MPSC. Accordingly, the studied five basic dyes can be approximately divided into three groups: (I) MC, which has a small molecular size; (II) FB and RB, which have middle sizes; and (III) BY and VB with large molecular sizes. The

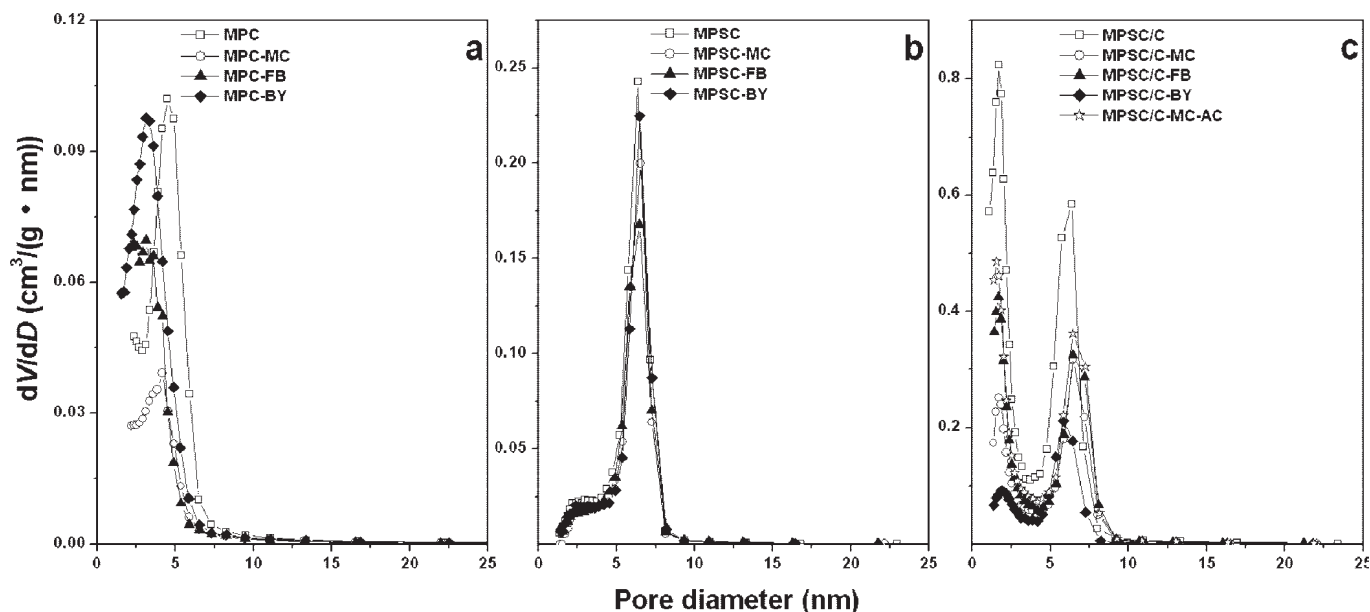


Figure 4. Pore size distributions for fresh mesoporous carbons and carbons after adsorption of MC, FB, and BY dyes and subsequent dilution by acetic acid: (a) MPC, (b) MPSC, and (c) MPSC/C.

Table 3. Adsorption Capacities for Dye Molecules on Ordered Mesoporous Carbons and Activated Carbon

dye	Q_e (mg/g)			
	AC	MPSC/C	MPC	MPSC
methylthionine chloride	396	758	540	384
fuchsin basic	362	689	207	371
rhodamine B	423	785	215	281
brilliant yellow	284	688	131	139
victoria blue B	222	210	83	106
methyl orange	392	637		
Sudan G	208	359		

adsorption quantities on mesoporous carbons are in the order of $\text{MPSC/C} > \text{MPC} > \text{MPSC}$ for group I; $\text{MPSC/C} > \text{MPSC} > \text{MPC}$ for group II; and $\text{MPSC/C} > \text{MPC} \approx \text{MPSC}$ for group III. These results demonstrate that the adsorption properties for dyes are sensitively dependent on the pore properties and dye molecular sizes.

3.3. Estimation on Pore Occupation. The XRD patterns for all mesoporous carbons after adsorption of the above dyes (here MC, FB, and BY are used as representative dyes) show a strong 10 reflection (Figure 1). The diffraction peak has almost the same position as that in the fresh samples, only a decrease in the intensity, indicating the same cell parameters (Table 2). These phenomena imply the adsorption of dye molecules inside pore channels of mesoporous carbons and negligible influence on the mesostructure.⁴⁸

The utilization of pores is estimated by the simple calculation of dye volume on the basis of the Newtonian ball and spring model. The estimated occupied pore volumes of MPC are 0.64, 0.19, 0.28, 0.12, and 0.09 cm^3/g after adsorption of MC, FB, RB, BY, and VB, respectively. Although the estimation is rough, it is clear that the highest adsorbed amount occurs for the basic MC dye with a small molecular size. The adsorbed MC molecules occupy the pore space, including micropores and mesopores. Although the adsorption amounts for dyes with larger sizes (such as FB and RB) decrease, corresponding to reduced occupied volumes. The reduction in occupied space becomes more

predominant in the cases of adsorbing BY and VB with the largest molecular sizes. Only about 20% of pores of MPC are utilized.

N_2 sorption isotherms were also used to investigate the occupied pore volume of mesoporous carbon after dye adsorption (Figure 8). Typical type IV curves are observed for all cases, further indicating that the mesopore structure can be retained. After adsorption of MC, the capillary condensation at middle relative pressures for MPC is indistinct (Figure 3a). The pore volume decreases from 0.55 to 0.15 cm^3/g , which is about 73% reduction in the total volume; and the value for the decrease in the specific surface area is about 78%. Simultaneously, micropores cannot be detected on the basis of the t -plot analysis. After FB adsorption, the capillary condensation step in the N_2 sorption isotherms is more distinct than that for MPC-MC but not as distinct as that in the fresh MPC sample. Accordingly, the adsorbed amount of nitrogen, and simultaneously the specific surface area and pore volume are higher than MPC-MC and lower than the fresh MPC. About 44% pores are occupied, close to the calculation from the Newtonian ball and spring model. The pore size distribution is wider, and the mostly possible value (3.1 nm) is smaller than that for the fresh MPC. The micropore volume is very low. MPC-BY displays a distinct capillary condensation step, a high surface area of 687 m^2/g , and a large pore volume of 0.47 cm^3/g , which are close to the fresh MPC. The utilization of pore space is 15%, in good agreement with the above dye-adsorption estimation.

The mesoporous carbon MPSC has 1.2, 1.10, 0.59, 0.22, and 0.21 mmol/g of adsorption amounts for MC, FB, RB, BY, and VB, respectively, which are roughly corresponding to 0.46, 0.35, 0.37, 0.13, and 0.12 cm^3/g of occupied volumes. N_2 sorption isotherms shows an increase for the adsorbed volume at the middle relative pressures in the order of fresh $\text{MPSC} > \text{MPSC-BY} > \text{MPSC-FB} \approx \text{MPSC-MC}$ (Figure 3b). After adsorption of MC and FB, the BET surface areas and pore volumes reduce to about 60 and 73% of those



Figure 5. Optical photographs for dye-polluted water (a, c, e) before and (b, d, f) after adsorption by the mesoporous carbon MPSC/C: (a, b) basic dye methylthionine chloride (MC), (c, d) basic dye fuchsin basic (FB), and (e, f) acidic and azo dye methyl orange (MO).

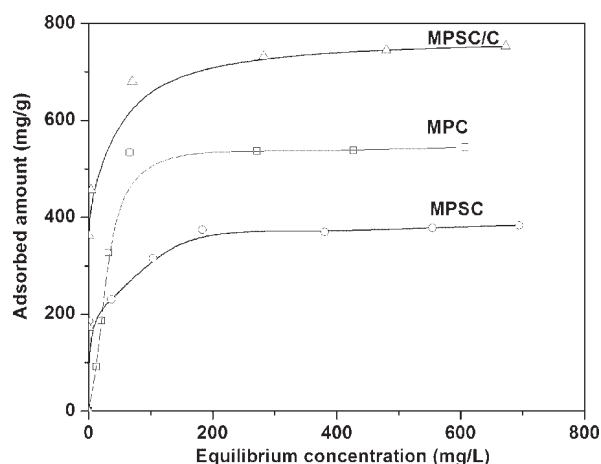


Figure 6. Adsorption isotherms for methylthionine chloride (MC) on ordered mesoporous carbonaceous adsorbents with various pore textural properties.

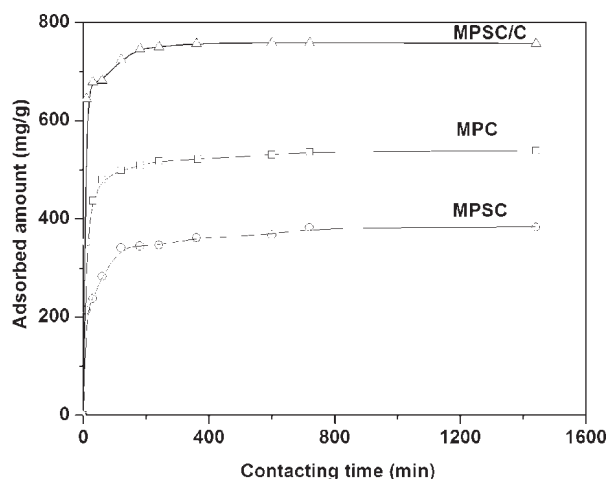


Figure 7. Adsorption capacities for MC on various ordered mesoporous carbonaceous materials (MPC, MPSC, and MPSC/C) as a function of the contacting time.

for the fresh carbon, respectively, indicating the packing of the MC and FB molecules inside the mesopore channels with a large size (6.4 nm). By comparison, the occupied pore surface area and pore volume after BY adsorption is lower, of 114 m²/g and 0.1 cm³/g, respectively.

The pore occupation of MPSC/C by basic dyes estimated from the Newtonian ball and spring model is 0.90, 0.65, 1.04, 0.64, and 0.23 cm³/g for MC, FB, RB, BY, and VB, respectively. The occupied volumes by dyes (MC, FB, RB,

Table 4. Desorption Data for the Ordered Mesoporous Carbon MPSC/C after Adsorption Methylthionine Chloride by Using Distilled Water, H₂SO₄, or Acetic Acid As a Desorbing Medium

desorbing medium	percent desorption (%)		
	1st run	2nd run	total
water	0.0	0.0	0.0
H ₂ SO ₄ (1 M)	2.6	2.1	4.6
acetic acid (50% V/V)	39.0	46.7	67.4

and BY) distinctly exceed the primary mesopore volume (0.51 cm³/g) in MPSC/C. Therefore, the involvement of dyes in small secondary mesopores is possible. The sharp increase in the nitrogen adsorption in the middle relative pressures (0.5–0.7) for MPSC/C reduces after dye adsorption (Figure 3c). At the same time, the increase in the p/p_0 range between 0.1 and 0.3 dramatically decreases. These phenomena, together with the large adsorption amount, reflect the occupation by dyes in both primary and secondary mesopores and the adsorption in secondary mesopores is predominant. The corresponding pore utilization exceeds 50%.

Activated carbon in which mesopores (ranging 1.5–30 nm) contribute total pore volume and surface area shows 32, 23, 39, 18, and 16% occupied volume after adsorption of MC, FB, RB, BY, and VB, respectively. These results suggest that the pore occupation by dyes with different sizes is closely related with the pore diameter and volume of the adsorbent.

3.4. Desorption. Table 4 shows the percent desorption of dye in various desorbing media. Desorption with distilled water cannot be found for MC on MPSC/C, indicating the occurrence of very small physisorption involving weak bonds attachment between MC and MPSC/C. Desorption of MC with 1.0 M H₂SO₄ is about 4.6%, indicating a small possibility of ion exchange in the adsorption process. Around 67.4% desorption of MC with acetic acid by twice desorption is obtained, indicating the selective desorption and chemisorption for most of dyes. This result is in accordance with the Langmuir adsorption isotherm.

The XRD pattern for the MPSC/C after desorption in acetic acid shows a relatively strong diffraction peak, similar to the fresh sample, with the unchanged cell parameter of 12.2 nm. N₂ sorption isotherms also reveal the typical type IV curves with a bimodal pore-size distribution. The BET specific area and pore volume are calculated to be 1559 m²/g and 1.47 cm³/g, respectively, implying the partial recovery of the pore space, in good agreement with the incomplete

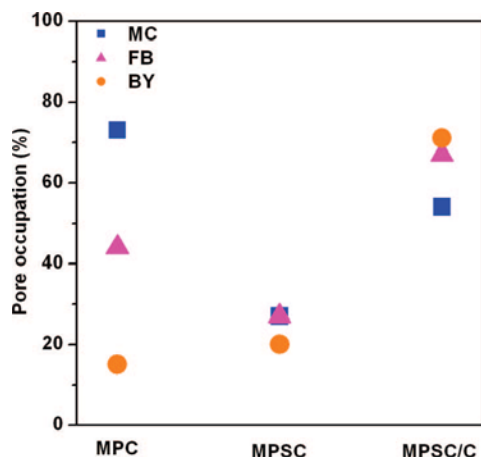


Figure 8. Estimated pore occupation after dye adsorption on the basis of N_2 sorption isotherms by the mesoporous carbonaceous adsorbents MPC, MPSC and MPSC/C with various textural properties. The symbols in the figures represent different adsorbing dyes: ■ MC, ▲ FB, and ● BY.

desorption. These results suggest that the adsorbent is stable and that the ordered mesostructure can be well-retained after dye adsorption and acetic acid elution.

4. Discussion

4.1. Highly Efficient Adsorption. Ordered mesoporous carbons with different pore textural properties that are prepared by using phenolic resins as carbon precursors via the surfactant-templating method show high adsorption capacities for multiple bulky dyes. The highest adsorption amount occurs on MPSC/C, which has a bimodal pore size, the largest pore volume, and the highest surface area. The highly efficient adsorption is also reflected by the high adsorption rate for low-concentration dyes and complete decoloration of wastewater containing basic, acidic, or azo dyes. The ordered mesostructure is stable after adsorption and elution, indicative of reusability.

4.2. Adsorption in Secondary Pores. The mesoporous carbons are derived from the same phenolic resins precursors and directly used without any further treatment. Almost a double (even three or four times) adsorption amount for all studied basic dyes on the MPSC/C adsorbent is detected on comparison with that on MPSC. This phenomenon is interesting because the two mesoporous carbons have the same primary but different secondary mesopores. The large difference may lie in the adsorption in these small secondary mesopores. A question here is the utilization of the small secondary mesopores with a mostly possible size below 2 nm in MPSC/C. We attribute the adsorption in these small mesopores to the interpenetrated pore system in the whole material. The mesopores are voids generated by etching silica inside the pore walls, and therefore are short, interpenetrated, and accessible.⁶⁶ The capillary force inside the secondary mesopores facilitates the mass transfer of dyes that are involved in the primary mesopores. Therefore, dye adsorption occurs in these small mesopores, which enhances the total adsorption capacity. A schematic diagram for the efficient adsorption in bimodal pores is shown in Figure 9. Although the density for the solid adsorbent changes after silica etching, the difference in

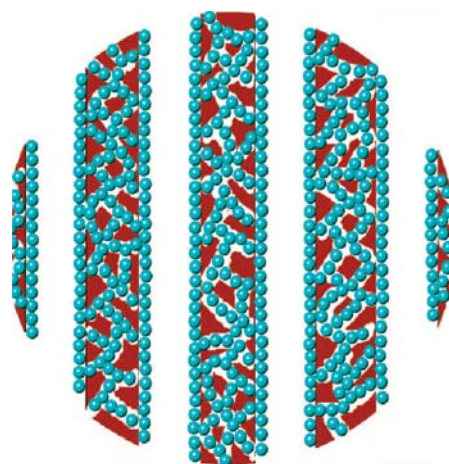


Figure 9. Schematic diagram for the dye adsorption on the ordered mesoporous carbon MPSC/C with interpenetrated bimodal pores.

density between silica and carbon is about 1.2 times, much lower than the difference in adsorption capacity. Therefore, the adsorption in secondary mesopores instead of the variation in pore wall density contributes the high adsorption performance. Another phenomenon is worth noting. MPSC/C exhibits an 85% adsorption in the first 10 min, whereas this value is about 56% for MPSC. Therefore, the secondary mesopores with short length may be responsible for the fast adsorption in MPSC/C.

The MPC adsorbent shows a high adsorption amount for small-molecule-size MC and high pore utilization. Because the major pore volume and surface area for MPC are contributed from micropores, the results also imply the adsorption of dyes in micropores. The micropores are generated from the release of small molecules during the carbonization of Bakelite resin, and hence, are interpenetrated with the mesopores. As a result, the capillary force is responsible for the dye adsorption in the micropores that first diffuse into primary mesopores.

4.3. Spatial Effect of Dye. As mentioned above, a small molecule (such as MC) can easily enter into the mesopores and micropores of MPC and MPSC/C, leading to a free mass transportation and high adsorption capacities. MPSC has only large primary mesopores and almost no micropores, and hence, mass transportation of MC inside pores should not be inhibited.

Both the capacity and the pore occupation for MPC decrease when adsorbing middle-size bulky dye molecules (FB and RB). But the values are predominantly larger than those after the adsorption of BY and VB with large molecular sizes. It has been reported that the pore blockage may occur due to the aggregation of large molecules in the orifice of small pores.^{3,41} The surface in the pores with small diameters cannot be fully utilized in adsorption. Therefore, the micropores easily undergo the aggregation of large molecules at the pore orifice, inhibiting further mass transportation. The adsorption for FB may principally occur in the primary mesopores while the secondary micropores are blocked. The low micropore volume of MPC-FB (after adsorption of FB on MPC) may reflect this result. Even small nitrogen molecules cannot go through micropores because of the orifice blockage. This

deduction is supported by the wide pore-size distribution and small pore size for MPC-FB. The coverage of the pore surface may also depend on the length of the diffusion path.⁵⁷ The particle sizes for all mesoporous carbon adsorbents are almost the same, about 10 μm (see Figure S5 in the Supporting Information), indicative of a long diffusion path. Therefore, the orifice blockage, together with the long diffusion path in MPC, is possibly responsible for the inefficient adsorption of large-size dyes. The utilization of pores in MPSC and MPSC/C after adsorption of group II dyes almost remains unchanged (sometimes even higher because of the larger dye molecular sizes) on comparison with that after MC adsorption. Bulky dye molecules are more likely sufficiently adsorbed in the large mesopores because of the free transportation. In addition, plenty of interpenetrated voids with a mostly possible size of 1.7 nm inside the pore walls in the MPSC/C adsorbent are large enough for the adsorption of FB and RB molecules. The pore blockage at the orifice may not occur. The voids facilitate the mass transfer, leading to a large adsorption amount.

For the dye molecules with large sizes (such as BY and VB, group III), the mesoporous MPC adsorbent shows low adsorption amounts, implying that the diffusion in primary mesopores with a small diameter is seriously inhibited when adsorbing large dye molecules. The occupation of pores and adsorption capacity are extremely low. Although the MPSC adsorbent has a large mesopore size, it undergoes a dramatic decrease in the adsorption capacity and occupied volume, similar to the MPC adsorbent. This phenomenon may be related to the long diffusion path in MPSC. The mesopores can not be fully accessed by large dye molecules. The MPSC/C adsorbent has a relatively high adsorption amount of BY, and the pore utilization is similar to that for the adsorption of small-molecule-size dyes, suggesting that the short, interpenetrated secondary mesopores can be utilized for the adsorption. However, the adsorption of VB on MPSC/C is inhibited. The pore occupation reduces. BY has a long chain, whereas VB is bulky in three dimensions. These phenomena indicate that the hindrance for adsorption of large molecules on MPSC/C is more distinct with a large size in three dimensions than with a long chain. The spatial effect of basic dye molecules is therefore the determinative factor for adsorption.

It should be noted that the pore occupation percentage after adsorbing the MC dye with a small molecular size on MPSC/C is lower than that on MPC despite the large adsorption amount of the former. The adsorption of the MC dye on carbon belongs to the Langmuir model. Although the pore surface of MPSC/C can be fully covered, a lot of pore space is unoccupied because of the large-size primary channels (6.4 nm). Similarly, the MPSC adsorbent shows a lower adsorption amount of MC than the MPC adsorbent with a large diameter, which has the similar pore volume with the latter. Plenty of pore space is unoccupied in MPSC. The lower surface area for MPSC may be responsible for

the lower adsorption amount on comparison with the MPC adsorbent. This phenomenon can also be observed on the mesoporous activated carbon adsorbent. The pore occupation is 32% after adsorption of MC. The pore size distribution for activated carbon is wide, ranging from 1.5 to 30 nm. The large pores cannot be fully filled. Therefore, when mass transportation is not inhibited, the adsorbent with a small pore size, a large pore volume, and a high surface area is desired.

5. Conclusions

Highly efficient adsorption of bulky dyes in wastewater has been demonstrated on ordered mesoporous carbon adsorbents prepared from the surfactant-templating approach. Our results show that ordered mesoporous carbon adsorbents have high adsorption rates (>99.9%) for low-concentration dyes, good performance in decoloration regardless of the dye nature, including basic, acidic, or azo dyes, and high stability after dye elution. In particular, the ordered mesoporous carbon MPSC/C adsorbent which has interpenetrated bimodal pores (6.4 and 1.7 nm), an extremely high surface area (2580 m^2/g), and a large pore volume (2.16 cm^3/g) exhibits higher capacities (about twice) in adsorbing bulky dyes than activated carbon. To establish the relationship between the size of adsorbate and pore size of adsorbent, we synthesized ordered mesoporous carbons with the same 2D hexagonal mesostructure but different pore textural properties by using phenolic resins as carbon sources and triblock copolymer F127 as a template. The spatial effect of dye molecules is the determinative factor for the adsorption in ordered mesoporous carbons. When adsorbing small-size dye molecules, the mesoporous adsorbent with small pore size, large pore volume, and high surface area is efficient. The pore utilization is high. In the cases of adsorption of large-molecule-size dyes, the adsorbent with large pore size, large pore volume, and high surface area is a good candidate. These behaviors offer good opportunities for mesoporous carbons in adsorption of organic pollutants.

Acknowledgment. This work was supported by NSF of China (20873086 and 20521140450), the program for New Century Excellent Talents in Universities (NCET-07-0560), and Shanghai Science & Technology and Education Committee (07QH14011, 07SG49, 07DZ22303, and 08JC-1417100).

Supporting Information Available: Synthesis procedure for carbon precursors; adsorption capacities from activated carbons in literatures; TG curves for mesoporous carbons prepared from the surfactant-templating method; $V-t$ plots for fresh mesoporous carbons and these carbons after dye adsorption; scheme for the generation of secondary mesopores in the MPSC/C adsorbent; N_2 sorption isotherms and $V-t$ plot analysis for activated carbon; representative low-magnification TEM image for mesoporous carbon adsorbents (PDF). This material is available free of charge via the Internet at <http://pubs.acs.org>.

CM8028577